Submitted to J. of Atmos. Sci., Nov 14, 2000; revised version submitted June 25, 2001

Possible aerosol effects on ice clouds via contact nucleation

Ulrike Lohmann

Atmospheric Science Programme, Department of Physics, Dalhousie University, Halifax, N.S., B3H 3J5, Canada. (Ulrike.Lohmann@Dal.Ca)

Abstract. The indirect effect of aerosols on water clouds, whereby aerosol particles change cloud optical properties, is caused by aerosol induced changes of the size and number of cloud droplets. This affects the lifetime of the water clouds as well as their shortwave radiative properties. In addition anthropogenic aerosols may change the properties of ice forming nuclei. To investigate the potential effect of aerosol-ice cloud interactions by contact freezing a prognostic equation for the number concentration of ice crystals is introduced into the ECHAM GCM. A simulation in which the number of contact ice nuclei is considered to be only temperature dependent is compared to simulations in which contact ice nuclei are considered to be dust aerosols. If dust aerosols are assumed to lose their nucleability by forming an internally mixed aerosol with sulfate, then the ice formation is slightly inhibited. On the contrary, if all contact nuclei are assumed to be insoluble carbonaceous aerosols, as found in contrails and some cirrus clouds, then contact nucleation is more important so that the liquid water path is smaller and the ice water path larger. These changes are, however, small compared to the extreme assumptions of having either no ice nuclei at all or so many ice nuclei that no supercooled cloud water exists.

1. Introduction

Anthropogenic aerosols such as sulfate and carbonaceous aerosols have substantially increased the global mean burden of aerosols from preindustrial times to the present-day. The indirect aerosol effect, where anthropogenic aerosols act as cloud condensation nuclei (CCN) thereby determining the initial cloud droplet number concentration (CDNC), albedo, precipitation formation, and lifetime of warm clouds is estimated to be between 0 and -2 W m^{-2}, e.g. Rotstayn (1999); Lohmann et al. (2000).

During the second Aerosol Characterization Experiment (ACE2) and during the Indian Ocean Experiment (INDOEX) it was found that the addition of anthropogenic aerosols increases the number of cloud droplets and decreases the mean cloud droplet size, e.g. Pawlowska and Brenguier (2000), Heymsfield and McFarquhar (2000). Experimentally it was found that the freezing temperature of cloud droplets depends on their volume (Pruppacher and Klett 1997) such that smaller droplets freeze at a lower temperature than larger droplets. Thus the decrease of cloud droplet size could lead to a slower or less frequent glaciation of supercooled clouds. This could, however, be offset because the probability of freezing rises as the number of cloud droplets increases. Therefore, a change in freezing behaviour due to anthropogenic aerosols could potentially change the phase of clouds and the long-

wave cloud radiative forcing. In current climate models, changes in homogeneous freezing cannot be simulated because saturation adjustment schemes are used. However, the parameterization of heterogeneous freezing that is used in Lohmann et al. (2000) depends on cloud droplet size and number, and thus could have been affected by changes in aerosol load. This effect was found to increase the global mean longwave radiation by only 0.2 W m^{-2} in Lohmann et al. (2000) which is comparable to the increase of 0.1 W m^{-2} in Rotstayn (1999).

Anthropogenic aerosols may also change the properties of ice forming nuclei. Precipitation originating from supercooled liquid water clouds where the temperatures are too warm for homogeneous freezing of cloud drops to occur requires an aerosol surface to provide a substrate for ice initiation. Typical natural ice nuclei in the atmosphere are insoluble particles like mineral and soil dust. They may lose their nucleability, if foreign gases such as sulfur dioxide (SO_2) or ammonia (NH_3) occupy their active sites (Pruppacher and Klett 1997).

Here the hypothesis that anthropogenic sulfur compounds reduce the nucleability of ice forming nuclei, which are assumed to be dust aerosols, is investigated. SO_2 adsorbed on a dust particle will occupy its active sites. Additionally, if oxidized to sulfate, the mixed aerosol will be hygroscopic and be incorporated in a cloud drop, and thus no longer be available as a contact nuclei. It could increase the number of immersion nuclei because the sulfate/dust mixture will have a surface for ice nucleation. However, the parameterization of immersion freezing currently used in ECHAM does not depend on the number of immersion freezing nuclei. Therefore only the change in the number of contact nuclei due to internally mixed sulfate/dust aerosols is considered.

In order to study aerosol-induced changes in ice clouds, first a prognostic equation for the number concentration of ice crystals is introduced (section 2) so that now the first two moments of the cloud droplet and ice crystal size distributions are predicted. Validation with observations is discussed in section 3. Three sensitivity experiments are conducted, including one in which the number of contact nuclei equals the number of dust aerosols, one where the number of contact nuclei is reduced in proportion to the number of sulfate aerosols to mimic an internally mixed sulfate-dust aerosol and one where all contact nuclei are assumed to be insoluble carbonaceous particles (section 4). Furthermore, two sensitivity experiments are carried out to test the most extreme assumptions about ice nuclei, either that ice nuclei are as abundant as cloud condensation nuclei so that no supercooled cloud water exists or that there are no ice nuclei at all. Section 5 summarizes the results and concludes this paper.

2. Model Description

The ECHAM model used in this study is a modified version based on Lohmann et al. (1999a). Prognostic aerosol variables are mass mixing ratios of sulfate, organic and black carbon, sub- and supermicron dust (0-1 μm and 1-2 μm), and sub- and supermicron sea salt (0-1 μm and 1-10 μm). Sulfate, organic and black carbon are as described in Lohmann et al. (1999a) except that the exponential aging time, where a hydrophobic carbonaceous aerosol becomes hydrophilic, has been reduced to 24 hours. Also, the in-cloud scavenging has been changed such that instead of following Giorgi and Chameides (1986) who assume a constant liquid water content of 0.5 g m^{-3}, here the model predicted liquid water content is used. The mineral dust fluxes are provided by (Ginoux et al. 2000) and the sea salt fluxes are based on the formulation by Monahan et al. (1986).

The prognostic cloud variables, mass mixing ratios of cloud liquid water and cloud ice, and the number concentrations of cloud droplets, are described in Lohmann and Roeckner (1996) and Lohmann et al. (1999a). The condensation/deposition parameterization has been changed and is now formulated using a better numerical scheme following Lenderink et al. (2000). Here a modified version of the Ghan et al. (1993) parameterization for cloud droplet nucleation that was derived using data from the North Atlantic Regional Experiment (NARE) is used at cloud base (Leaitch et al. 1996), (Lin and Leaitch 1997):

$$Q_{nucl} = \max\left[\frac{1}{\Delta t}\left(0.1(N_l^{max})^{1.27} - N_{old}\right), 0\right] \qquad (1)$$

where

$$\mathrm{N_l^{max}} = \frac{\mathrm{N_a w}}{\mathrm{w} + \alpha \mathrm{N_a}} \qquad (2)$$

and $\alpha = 0.023$ cm^4 s^{-1}. N_a is the number concentration of the sum of sea salt, hydrophilic black carbon, hydrophilic organic carbon, ammonium sulfate, methane sulfonic acid and 10% of the dust aerosols

that is assumed to be hydrophilic. Here an externally mixed aerosol is assumed. The updraft velocity w is obtained as the sum of the grid mean vertical velocity and a turbulent contribution expressed in terms of the turbulent kinetic energy (TKE) for stratiform clouds (Lohmann et al. 1999a) and in terms of the convectively available potential energy (CAPE) for convective clouds (Leo Donner, personal communication, 1999):

$$w = \begin{cases} \overline{w} + 1.33\sqrt{TKE} & \text{stratiform clouds} \\ \overline{w} + 0.5\sqrt{CAPE} & \text{convective clouds} \end{cases} \quad (3)$$

Note that the scaling factor in (3) used here for stratiform clouds is almost twice as large as described in Lohmann et al. (1999a). The higher factor is necessary because the maximum number of cloud droplets activated is determined first (equation (2)). It corresponds roughly to the 5% highest updraft velocities found during NARE. Then the maximum cloud droplet number is empirically related to the average cloud droplet number concentration in equation (1).

Nucleation is only calculated at cloud base when condensation occurs. The amount of droplets nucleated is assumed to be constant throughout the depth of the cloud to mimic the internal circulation inside the cloud. In old clouds, only new droplets are formed if the number that would be activated at cloud base exceeds the number of pre-existing cloud droplets at cloud base (N_{old}).

Most importantly, a prognostic equation for the number concentration of ice crystals (N_i) is introduced:

$$\begin{aligned} \frac{\partial N_i}{\partial t} &= R(N_i) + Q_{\text{nuci}} - Q_{\text{mlt}} + \frac{N_i}{q_i}(Q_{\text{frz}} + Q_{\text{secp}} \\ &\quad - Q_{\text{agg}} - Q_{\text{saci}} - Q_{\text{self}} - Q_{\text{sub}}) \end{aligned} \quad (4)$$

$R(N_i)$ represents the advective, turbulent, and convective transports of N_i. Convective transport refers to the detrainment at the top of cumulus clouds. For convectively detrained ice crystals as well as for ice crystals formed at temperatures below -35°C (Q_{nuci}), the number concentration of ice crystals is related to the newly formed ice water content (q_i^{new}) as tested in the column model version of the Canadian climate model (Lohmann et al. 1999b). First of all the effective ice crystal radius r_{ie} is determined. It is parameterized as a function of temperature based on observations from mid-latitude cirrus by Ou and Liou (1995) (in SI units):

$$\begin{aligned} r_{ie} &= 0.5 \cdot 10^{-6} \, [326.3 + 12.4 \, (T - T_o) \\ &\quad + 0.2 \, (T - T_o)^2 + 0.001 \, (T - T_o)^3] \end{aligned} \quad (5)$$

where T_o=273.16 K.

Then the mean volume radius r_{iv} is determined by empirically relating it to the effective ice crystal radius r_{ie} from simultaneous measurements of the two radii (Moss, personal communication, 1996):

$$r_{iv} = 10^{-6} \sqrt[3]{\beta + \sqrt[3]{\gamma + \delta \cdot r_{ie}^3}} \quad (6)$$

where $\beta = -2.261 * 10^3$, $\gamma = 5.113 * 10^6$ and $\delta = 2.809 * 10^3$.

With that the rate at which new ice crystals nucleate is given as

$$Q_{nuci} = \frac{3\rho_0 q_i^{new}}{4\pi\rho_i \, r_{iv}^3} \cdot \frac{1}{\Delta t} \quad (7)$$

where ρ_i ($= 500 \; kg \; m^{-3}$) is the ice crystal density, ρ_0 is the air density, Δt is the model timestep and q_i^{new} refers to either the detrained cloud ice mass mixing ratio or the cloud ice mass mixing ratio calculated from the saturation adjustment scheme used for deposition.

The other microphysical processes are aggregation of ice crystals Q_{agg}, self-collection of ice crystals Q_{self}, accretion of ice crystals by snow Q_{saci}, freezing of cloud droplets Q_{frz} and secondary production of ice crystals Q_{secp} (see below), melting of ice crystals Q_{mlt}, and sublimation of ice crystals Q_{sub}. The conversion rates in terms of the cloud ice mass mixing ratio are described by Lohmann and Roeckner (1996). They are adapted from the mesoscale model GESIMA (Levkov et al. 1992). For all processes except nucleation and melting, it is assumed that the ice crystal number concentration is depleted in proportion to the ice water mixing ratio following Levkov et al. (1992). In case of sublimation, this should mimic heterogeneous sublimation where some ice crystals from all size categories sublimate. Evidence for heterogeneous evaporation has been observed for cloud droplets (Hudson and Rogers 1986).

The ice phase in ECHAM can be initiated by immersion and condensation freezing, contact freezing or deposition. The only parameterization of heterogeneous

ice formation between -35°C and 0°C which depends on the number of ice nuclei is contact freezing of cloud droplets (m^{-3} s^{-1}) following Levkov et al. (1992) (in SI units):

$$Q_{frz,cnt} = m_{io} D_{ap} 4\pi r_l N_{a,\mathrm{cnt}} \frac{N_l^2}{\rho q_l} \qquad (8)$$

where r_l is the volume mean droplet radius, q_l is the cloud liquid water mass mixing ratio in the cloudy part of the grid box, N_l is the number concentration of cloud droplets, ρ is the air density, T is the temperature, m_{io} = 10^{-12} kg is the original mass of a newly formed ice crystal, D_{ap} is the Brownian aerosol diffusivity, $N_{a,\mathrm{cnt}}$ is the number of contact nuclei following Young (1974) given as $N_{ao}(270.15 - T)^{1.3}$ where N_{ao} = 2×10^5 m^{-3} is the number of active ice nuclei at 269.15 K. In the reference simulation, N_{ao} is assumed to be constant with height following Cotton et al. (1986). The Brownian aerosol diffusivity is given by:

$$D_{ap} = \frac{kTC_c}{6\pi\eta r_m} \qquad (9)$$

where k is the Boltzmann constant, T is the temperature, η is the viscosity of air ($\eta = 10^{-5}$ (1.718+0.0049*(T-T_o)-1.2*10^{-5}*(T-T_o)^2) kg m^{-1} s^{-1}), r_m is the aerosol mode radius and C_c is the Cunningham correction factor (C_c = 1+1.26 $\frac{\lambda}{r_m}\frac{p_o}{p}\frac{T}{T_o}$). Here λ is the molecular free path length of air (λ=0.066 μm) and p_o and T_o refer to standard condition of 101325 Pa and 273 K. The aerosol mode radius is taken to be 0.01 μm in the standard simulation.

Immersion and condensation freezing is given by Levkov et al. (1992) based on the laboratory data from Bigg (1953):

$$Q_{\mathrm{frz,imm}} = a[\exp\{b(273.2 - T)\} - 1]\frac{\rho q_l}{\rho_l} \qquad (10)$$

where a=100 m^{-3} s^{-1}, b=0.66 K^{-1} and ρ_l is the water density.

Secondary ice production uses a parameterization of the Hallett-Mossop process that takes place between -3°and -8°C as described in Levkov et al. (1992):

$$Q_{\mathrm{secp}} = K(1 - f_{25}J) \qquad (11)$$

where K (=0.003) is a temperature dependent coefficient, f_{25} is the fraction of cloud droplets smaller than 25 μm and J is the rate of collisions between the snow crystals and cloud droplets greater than 25 μm in diameter given by:

$$J = \frac{E_{sw}\pi\rho q_w n_{0S}\Gamma(3.5)}{4\lambda_s^{3.5} m_w}\left(\frac{4g\rho_s}{3C_D\rho}\right)^{0.5} \qquad (12)$$

where m_w (=4.19 10^{-12} kg) is the mean cloud droplet mass treating the cloud water as monodisperse, E_{sw} is the collection efficiency of snow for cloud water, which is assumed to be 1, g is the acceleration by gravity, ρ_s (=0.1 kg m^{-3}) the density of snow, and C_D (=0.6) is the drag coefficient.

3. Comparison with Observations

All simulations were conducted in T30 horizontal resolution with 19 vertical levels over a period of 3 years after an initial spin-up of 3 months. Satellite retrievals of cloud ice are not yet available, so the only data sets that can be used for model validation are those obtained during field campaigns. Figure 1 shows the average cloud water content versus in-cloud temperature measured by aircraft (Learjet) during the Central Equatorial Pacific Experiment (CEPEX) between 20°S and 2°N, and between 165°E and 170°W (Lohmann et al., 1995; McFarquhar and Heymsfield, 1996). Vertical bars indicate the 25% and 75% quartiles of the observations. The average ice water content during CEPEX is dominated by a few cases with large ice water contents, because the ice water content in each temperature bin is positively skewed. It can, therefore, exceed the 75% percentile value (Fig. 1). In addition exponential fits of the ice water content as a function of in-cloud temperature from 4 different field experiments (Heymsfield 1993) in the midlatitudes and tropics have been added. Since the observational data probably include supercooled cloud droplets, the sum of cloud ice and supercooled cloud water is taken from the model simulation as well as only the ice water content. The model data are sampled every 12 hours for one month between 50°N and 50°S. ECHAM captures the observed increase of condensed water with temperature as evident in all data sets. However, the ice water content alone has its maximum value between -25°C and -20°C and decreases at warmer temperatures.

Figure 2 shows the percentage of liquid water found in clouds between 0 and -40°C from the same model data. Superimposed are best fits to observations from the British Isles (Moss and Johnson 1994) and from Russia (Matveev 1984). The observations made with the British aircraft show that no liquid water exists below -10°C whereas the data over the Russia as well as recent observations in the Arctic (Bretherton et al. 2000) show that supercooled cloud liquid water can exist at temperatures as low as -35 or -40°C. ECHAM falls in between the different estimates. It agrees better with

the observations over Russia and the Arctic in that supercooled water can be found at temperatures as low as -35°C.

4. Sensitivity Experiment

In the first sensitivity study, equation (8) is linked to the predicted aerosols by assuming that the number of active ice nuclei at 269 K equals the number of dust aerosols (simulation DUST). Here the temperature dependence that Young (1974) assumed for contact nuclei ($N_{a,\mathrm{cnt}} = N_{io}(270.15 - T)^{1.3}$) is kept. It takes into account the temperature dependence of dust contact nuclei that was found by Pitter and Pruppacher (1973) from wind tunnel studies. It also allows for volcanic or meteoric dust, which have not been taken into account, to additionally act as ice forming nuclei at higher altitudes or colder temperatures. The number of dust aerosols is obtained from the accumulation and coarse mode dust mass mixing ratio by assuming log-normal distributions with mode radii of 0.39 μm and 1.9 μm, a density of 2600 kg m^{-3} and a geometric standard deviation of 2 and 2.15, respectively (Hess et al. 1998). This is an upper bound for the number of natural contact nuclei, because an external mixture is assumed. That is, the dust aerosols are assumed to be free from contaminations by SO_2 or sulfuric acid.

In the second sensitivity study the number of dust contact nuclei is reduced according to the abundance of sulfate aerosols (simulation DUST-SULF). This is motivated by studies by Dentener et al. (1996) and Levin et al. (1996) based on observational data showing that Asian and Mediterranean mineral aerosols are often coated with sulfates and other soluble materials as well as on laboratory measurements showing that 25-400 mg SO_2 g^{-1} may be removed by fly ash, cement and dust. Although the heterogeneous reaction of SO_2 on mineral dust is highly unknown Dentener et al. (1996) accounted for it using a chemical transport model. They showed that the region from East Asia to the central Pacific Ocean had more than 10% of the sulfate associated with mineral dust. The reaction of SO_2 with dust was found to be so fast as compared to their reference simulation without dust that more SO_2 reacted to sulfate instead of being removed by dry deposition. Here sulfate is assumed to render the portion of the dust mass that corresponds to the sulfate mass inactive as contact nuclei evenly divided between the sub- and supermicron mode. Then the remaining dust mass is converted into the number of contact nuclei. As sulfate aerosols are mainly anthropogenic, this difference in contact nuclei could be taken as an estimate of the anthropogenic impact of sulfur coating of dust particles. In these two simulations the mode radius in the aerosol diffusivity is taken to be the mode radius of the accumulation size dust aerosols (0.39 μm).

Another extreme assumption is considered in simulation CARB where all contact nuclei are assumed to be insoluble carbonaceous particles (sum of hydrophobic black carbon and hydrophobic organic carbon). Here the temperature dependence that Young (1974) assumed for contact nuclei ($N_{a,\mathrm{cnt}} = N_{io}(270.15 - T)^{1.3}$) is kept as well. Evidence for carbonaceous material as ice nuclei was found in contrails and some cirrus clouds e.g. Schröder et al. (1998), Ström and Ohlsson (1998). For this simulation, the mode radius for the aerosol diffusivity is 0.016 μm.

Figure 3 shows the annually zonal averaged contact nuclei number concentration as a function of height from the reference simulations and the simulations DUST, DUST-SULF and CARB. In the reference simulation contact nuclei concentration increase strongly with decreasing temperature. They are most numerous around the tropical and polar tropopause. Dust contact nuclei, on the other hand, increase less strongly with height. They are more abundant in the polar middle and upper troposphere than in the lower troposphere showing the better nucleation behavior with decreasing temperature as found by Pitter and Pruppacher (1973). If an internal mixture of dust and sulfate is assumed, the ice nuclei concentration is only slightly reduced as compared to DUST. The contact nuclei concentration is highest in the northern hemisphere and in the tropics, if contact nuclei are assumed to be insoluble carbonaceous particles.

The large difference in the number of ice nuclei between the control simulation and the simulation DUST is not reflected in the difference in the number of ice crystals at temperatures between 0 and -35°C. Even though the concentration of contact nuclei is larger in the DUST simulation than that in the control simulation, ice crystals are more numerous in the polar mid troposphere in the control simulation caused by the smaller aerosol diffusivity in the DUST simulation. A slight reduction in ice crystal number concentration in DUST-SULF as compared to DUST is only evident near the surface in Antarctica. Even though there are 2 orders of magnitude more ice nuclei in simulation CARB in the north-

ern hemisphere mid-latitudes than in DUST, the ice crystal number has only slightly increased. As contact freezing depends quadratically on the cloud droplet number concentration, a faster contact freezing caused by more ice nuclei will decrease the cloud droplet number concentration. Subsequently fewer cloud droplets are available limiting the contact freezing process. The ice crystal number concentrations are similar to those predicted by Ghan et al. (1997) using the NCAR GCM.

The similarity of all simulations in the upper troposphere and lower stratosphere is caused by homogeneous freezing and deposition of water vapor onto the existing ice crystals below -35°C. This is the result of using a simple saturation adjustment scheme for homogeneous freezing. However, Kärcher and Lohmann (2001) and Lohmann and Kärcher (2001) showed that even if homogeneous freezing is parameterized as a function of vertical velocity and temperature and the saturation adjustment scheme is abandoned, homogeneous freezing is not limited by the number of hygroscopic aerosols. That is, anthropogenic aerosol and precursor emissions seem to have no effect on cirrus formed by homogeneous freezing.

Figure 3 also shows the different cloud droplet number concentrations for these simulations. In DUST and DUST-SULF, where contact freezing in the northern hemisphere mid and lower troposphere is smallest, the number of cloud droplets is higher than in the control experiment and CARB.

Figure 4 shows the annually zonal averaged liquid and ice water path and shortwave and longwave cloud forcing from the control simulation, DUST, DUST-SULF and CARB together with observations. Since the observations of liquid water path from the Special Sensor Microwave Imager (SSM/I) from Greenwald et al. (1993) and Weng and Grody (1994) are only available over the ocean, the comparison of liquid and ice water path is restricted to ocean points only.

The ice water path shows maxima in the intertropical convergence zone and in the stormtracks of the extratropics. The simulation DUST and DUST-SULF are very similar, the global mean ice water path is the same in both experiments (see also Table 1). The ice water path is everywhere highest in the control simulation followed by simulation CARB.

The liquid water path is highest in DUST and DUST-SULF and lowest in CARB. The difference in global mean liquid water path between CARB and DUST is 22 g m^{-2} (Table 1). As compared to the SSM/I observations the liquid water path is larger in all 4 simulations, especially the maximum in the tropics is larger by more than a factor of 2. As the longwave cloud forcing is underestimated and the shortwave cloud forcing overestimated in the tropics in all 4 simulations that might point to problems in the convection scheme rather than to problems in the large scale cloud scheme. The mass flux scheme used in this study, the Tiedtke convection scheme (Tiedtke 1989) together with the updates by Nordeng (1994), detrains most of the cloud water from shallow convective clouds and only a small fraction in anvils. That would lead to an overestimation of the liquid water path and shortwave cloud forcing and an underestimation of the longwave cloud forcing. Another explanation is that the convective clouds do not penetrate high enough in the troposphere. A thorough analysis of the convection scheme, however, is beyond the scope of this paper. The maxima in shortwave cloud forcing in mid-latitudes are best captured in simulations DUST and DUST-SULF as compared to CARB. This is reassuring as the former two assumptions are most realistic.

The globally annual mean averages are summarized in table 1. The difference between DUST and DUST-SULF could be thought of as the anthropogenic influence. In pre-industrial times, much fewer sulfate aerosols were present in the atmosphere and the external mixture assumption could have prescribed the number of contact nuclei well. In present-day times, anthropogenic emissions of sulfur dioxide will be oxidized to sulfate aerosols. If these aerosols or even sulfur dioxide come in contact with dust aerosols, they are likely to reduce the number of active sites. However, the differences between DUST and DUST-SULF in terms of the shortwave and longwave cloud forcing are only 0.2 and 0.1 W m^{-2}, respectively. So the sulfate coating of dust is not the most important factor for changing contact nucleation. Changes in aerosol size are more important as the diffusivity depends nonlinearly on size once the Cunningham correction factor is not negligible. This is the case if aerosols are comparable in size or smaller than the molecular mean free path.

To address the maximum impact aerosols could have on ice clouds, sensitivity experiments using extreme assumptions employing the simpler model set-up without number concentrations for ice crystals and cloud droplets as described in Lohmann and Feichter (1997) are performed. In simulation ICE it is assumed that

Table 1. Global annual mean liquid water path (LWP) (g m^{-2}), ice water path (IWP) (g m^{-2}), shortwave cloud forcing (SCF) (W m^{-2}), longwave (LCF) (W m^{-2}) and net cloud forcing (CF) (W m^{-2}) for the reference simulation (REF), the simulation DUST, DUST-SULF, CARB and observations of the cloud forcings from ERBE.

Exp	REF	DUST	DUST-SULF	CARB	ERBE
LWP	85.0	106.2	106.2	83.9	
IWP	20.8	18.7	18.7	20.2	
SCF	-45.8	-49.7	-49.9	-45.5	-49.1
LCF	30.8	33.2	33.3	30.7	29.7
CF	-15.0	-16.5	-16.6	-14.8	-19.4

no liquid water can exist below 0°C, that is, the atmosphere would have an abundance of ice nuclei at all subfreezing temperatures. On the other hand, in the simulation LIQUID it is assumed that all cloud droplets are supercooled down to -35°C, that is, no ice nuclei exist at all. The impact on liquid and ice water path as well as on the longwave and shortwave cloud forcing is shown in figure 5. The liquid water path in simulation LIQUID is three times larger than in the simulation ICE while the ice water path is only twice as large as in the simulation ICE compared to the simulation LIQUID in the global mean (see table 2). The smaller sensitivity in ice water path reflects the more efficient precipitation mechanism via the ice phase. The difference in total cloud water path has a profound impact on the radiation budget such that the shortwave and longwave cloud forcing are 17 W m^{-2} and 5 W m^{-2} larger in LIQUID than in ICE, respectively. The ICE simulation is closer to the reference simulation allowing for mixed-phase clouds (simulation MIX) indicating the rapid glaciation of supercooled clouds once a sufficient number of ice crystals has been formed.

Fowler and Randall (1996) performed a sensitivity study between a mixed phase cloud simulation allowing supercooled cloud water down to -40°C corresponding to our MIX simulation and a simulation with no supercooled clouds corresponding to our ICE simulation. They found larger differences of 8 W m^{-2} in both the longwave and shortwave cloud forcing probably because they did perpetual January simulations whereas here the full annual cycle is simulated.

The cloud phase has an impact on the indirect aerosol effect. For the simulations ICE and LIQUID pre-industrial simulations were also performed. In these simulations the fossil fuel emissions are set to zero and the biomass burning is reduced to 10% of the present-day value. The indirect aerosol effect is then taken to be the difference in shortwave cloud forcing between the present-day and pre-industrial experiment. While the indirect effect is -1.4 W m^{-2} in the reference simulation (Lohmann and Feichter, 1997) it is larger in LIQUID with -2.2 W m^{-2} and smaller in ICE with -1.1 W m^{-2}. The indirect effect is smallest in ICE because here the increase in liquid water path is only a third of that in LIQUID. The longwave cloud forcing, however, changes only by 0.1 W m^{-2} between pre-industrial and present-day times in all simulations.

Table 2. Global annual mean liquid water path (LWP), ice water path (IWP), shortwave cloud forcing (SCF) and longwave cloud forcing (LCF) for the simulations ICE and LIQUID and compared to the reference simulation with mixed phase clouds MIX

Experiment	ICE	LIQUID	MIX
LWP (g m^{-2})	55	160	63
IWP (g m^{-2})	27	14	26
SCF (W m^{-2})	-43	-60	-47
LCF (W m^{-2})	29	34	30

5. Summary and conclusions

The ECHAM model was used to investigate the sensitivity of contact freezing to assumptions in contact ice nuclei. A simulation, in which contact ice nuclei depend only on temperature were compared to simulations in which contact ice nuclei were assumed to be dust (simulation DUST) or insoluble carbonaceous aerosols (simulation CARB). The ice water path was reduced in DUST as compared to the reference simulation because the contact nucleation depends on the aerosol diffusivity which is strongly size dependent. As the dust nuclei are larger than the contact nuclei in the reference simulation the contact nucleation is less efficient in DUST.

Accounting for internally mixed aerosols rather than externally mixed aerosols, by reducing the number of contact nuclei in proportion to the mass of sulfate aerosols present as motivated by the study of Dentener et al. (1996), changes both the number of ice crystals and the ice water content only slightly. As sulfate aerosols are

mainly anthropogenic, this difference in contact nuclei could be taken as the anthropogenic impact on contact nucleation. In reality, some natural sulfate, nitrate or organics could have formed an internal mixture with dust and some dust in an internally mixed aerosol could act as an immersion nuclei which would reduce this effect even more.

As contact nucleation depends on the strongly size dependent aerosol diffusivity larger changes in ice clouds can be expected from anthropogenic emissions of smaller insoluble carbonaceous aerosols. The difference in ice water path in simulation CARB as compared to simulation DUST amounts to 1.5 g m^{-2}. This is accompanied by a 22.3 g m^{-2} difference in liquid water path. The difference in ice water path is smaller than in liquid water path because the precipitation formation via the ice phase is more efficient. The resultant change in cloud forcing is a 4.2 W m^{-2} smaller shortwave cloud forcing and a 2.5 W m^{-2} smaller longwave cloud forcing in CARB as compared to DUST.

These differences in liquid and ice water path are, however, much smaller than what has been assumed in two extreme sensitivity studies. Simulation LIQUID assumes that no ice nuclei exists above -35°C while simulation ICE assumes that ice nuclei are as abundant as cloud condensation nuclei and therefore no liquid water clouds exist below 0°C. Then the difference in liquid water path between these two simulations is 105 g m^{-2} and 13 g m^{-2} in ice water path.

Our attempt to account for the reduction in active sites on dust aerosols is very simplified. Here we depleted the dust mass in proportion to the sulfate mass whereas a thin sulfate coating may be sufficient. A more realistic way would be to explicitly simulate the uptake and oxidation of sulfur dioxide with ozone on dust aerosols as done by Dentener et al. (1996). In order to parameterize the absorption of SO_2 on dust aerosols, the concentration of HO_2 is needed as both HO_2 and SO_3^+ act as chain carriers. We currently do not prescribe HO_2 concentrations in the model. However, it should be addressed in future studies. Moreover, while we did not change the cloud droplet nucleation in this study to isolate the effect of contact nucleation, the impact of the internally mixed dust-sulfate aerosol on cloud droplet nucleation should be taken into account in future studies as well.

Contact nucleation is only one aspect in which anthropogenic aerosols can influence ice clouds. Other ways in which anthropogenic aerosols could influence ice clouds include 1) a reduction in the freezing point of cloud drops, 2) homogeneous freezing of sulfuric acid drops, and 3) other heterogeneous freezing mechanisms (immersion freezing and condensation freezing) which have not been considered here. Their impact could be much larger as the sensitivity experiments with extreme assumptions about the chemical composition of contact nuclei have shown.

Acknowledgments The author thanks Dean Hegg, Glen Lesins and Johann Feichter for helpful comments and suggestions. Ulrike Lohmann is grateful for support from the National Science and Engineering Research Council of Canada. Ulrike Lohmann also thanks the Deutsches Klimarechenzentrum for computing time. A preliminary version of this study was presented at the European workshop on Aviation, Aerosols, Contrails and Cirrus Clouds (A2C3), in Seeheim, Germany, July 10-12, 2000.

References

Bigg, E. K. 1953. The supercooling of water. *Proc. Phys. Soc.* **66**, 688–694.

Bretherton, C. S., de Roode, S. R., Jakob, C., Andreas, E. L., Intrieri, J., Moritz, R. E. and Persson, P. O. G. 2000. A comparison of the ECMWF forecast model with observations over the annual cycle at SHEBA. *J. Geophys. Res.* Subm. to.

Cotton, W. R., Tripoli, G. J., Rauber, R. M. and Mulvihill, E. A. 1986. Numerical simulation of the effects of varying ice crystal nucleation rates and aggregation processes on orographic snowfall. *J. Clim. Appl. Meteorol.* **25**, 1658–1680.

Dentener, F., Carmichael, G. R., Zhang, Y., Lelieveld, J. and Crutzen, P. J. 1996. Role of minearl aerosol as a reactive surface in the global troposphere. *J. Geophys. Res.* **101**, 22,869–22,889.

Fowler, L. D. and Randall, D. A. 1996. Liquid and ice cloud microphysics in the csu general circulation model. part iii: Sensitivity to modeling assumptions. *J. Climate* **9**, 561–586.

Ghan, S. J., Chuang, C. C. and Penner, J. E. 1993. A parameterization of cloud droplet nucleation, part i, single aerosol type. *Atmos. Res.* **30**, 197–221.

Ghan, S. J., Leung, L. R., Easter, R. C. and Abdul-Razzak, H. 1997. Prediction of cloud droplet number in a general circulation model. *J. Geophys. Res.* **102**, 21,777–21,794.

Ginoux, P., Chin, M., Tegen, I., Prospero, J., Holben, B., Dubovik, O. and Lin, S.-J. 2000. Sources and distributions of dust aerosols simulated with the GOCART model. *J. Geophys. Res.* Subm. to.

Giorgi, F. and Chameides, W. L. 1986. Rainout lifetimes of highly soluble aerosols and gases inferred from simulations with a general circulation model. *J. Geophys. Res.* **91**, 14,367–14,376.

Greenwald, T. J., Stephens, G. L., Vonder Haar, T. H. and Jackson, D. L. 1993. A physical retrieval of cloud liquid water over the global oceans using special sensor microwave/imager (SSM/I) observations. *J. Geophys. Res.* **98**, 18,471–18,488.

Hess, M., Koepke, P. and Schult, I. 1998. Optical properties of aerosols and clouds: The software package OPAC. *Bull. Am. Meteorol. Soc.* **79**, 831–844.

Heymsfield, A. J. 1993. Microphysical structures of stratiform and cirrus clouds. In: P. V. Hobbs, ed., *Aerosol-cloud-climate interactions*, Academic Press, San Diego, CA, vol. 54, chap. 4. 97–121.

Heymsfield, A. J. and McFarquhar, G. M. 2000. Microphysics of INDOEX clean and polluted trade cumulus clouds. *J. Atmos. Sci.* Subm. to.

Hudson, J. G. and Rogers, C. F. 1986. Relationship between critial supersaturation and cloud droplet size: Implications for cloud mixing processes. *J. Atmos. Sci.* **43**, 2341–2359.

Kärcher, B. and Lohmann, U. 2001. A parameterization of cirrus cloud formation:
homogeneous freezing of supercooled aerosols. *J. Geophys. Res.* Subm. to.

Leaitch, W. R., Banic, C. M., Isaac, G. A., Couture, M. D., Liu, P. S. K., Gultepe, I., Li, S.-M., Kleinman, L., MacPherson, J. I. and Daum, P. H. 1996. Physical and chemical observations in marine stratus during the 1993 north atlantic regional experiment: Factors controlling cloud droplet number concentrations. *J. Geophys. Res.* **101**, 29,123–29,136.

Lenderink, G., Meijgaard, E. v. and Holtslag, A. A. M. 2000. Numerical modeling of the atmosphere/continent system - evaluation of the ECHAM4 cloud-turbulence scheme for stratocumulus. *Meteorologische Zeitschrift* **9**, 41–48.

Levin, Z., Ganor, E. and Gladstein, V. 1996. The effects of desert particles coated with sulfate on rain formation in the eastern Mediterranean. *J. Appl. Meteorol.* .

Levkov, L., Rockel, B., Kapitza, H. and Raschke, E. 1992. 3D mesoscale numerical studies of cirrus and stratus clouds by their time and space evolution. *Beitr. Phys. Atmos.* **65**, 35–58.

Lin, H. and Leaitch, W. R. 1997. Development of an in-cloud aerosol activation parameterization for climate modelling. In: *Proceedings of the WMO Workshop on Measurement of Cloud Properties for Forecasts of Weather, Air Quality and Climate*. World Meteorol. Organ., Geneva.

Lohmann, U. and Feichter, J. 1997. Impact of sulfate aerosols on albedo and lifetime of clouds: A sensitivity study with the ECHAM GCM. *J. Geophys. Res.* **102**, 13,685–13,700.

Lohmann, U., Feichter, J., Chuang, C. C. and Penner, J. E. 1999a. Predicting the number of cloud droplets in the ECHAM GCM. *J. Geophys. Res.* **104**, 9169–9198.

Lohmann, U., Feichter, J., Penner, J. E. and Leaitch, W. R. 2000. Indirect effect of sulfate and carbonaceous aerosols: A mechanistic treatment. *J. Geophys. Res.* **105**, 12,193–12,206.

Lohmann, U. and Kärcher, B. 2001. First interactive simulations of cirrus clouds formed by homogeneous freezing in the echam gcm. *J. Geophys. Res.* Subm. to.

Lohmann, U., McFarlane, N., Levkov, L., Abdella, K. and Albers, F. 1999b. Comparing different cloud schemes of a single column model by using mesoscale forcing and nudging technique. *J. Clim.* **12**, 438–461.

Lohmann, U. and Roeckner, E. 1996. Design and performance of a new cloud microphysics scheme developed for the ECHAM general circulation model. *Clim. Dyn.* **12**, 557–572.

Lohmann, U., Roeckner, E., Collins, W. D., Heymsfield, A. J., McFarquhar, G. and Barnett, T. P. 1995. The role of water vapor and convection during the Central Equatorial Pacific Experiment from observations and model simulations. *J. Geophys. Res.* **100**, 26,229–26,235.

Matveev, L. V. 1984. *Cloud Dynamics*. D. Reidel Publishing Company, Dordrecht, The Netherlands.

McFarquhar, G. M. and Heymsfield, A. J. 1996. Microphysical characteristics of three cirrus anvils sampled during the central equatorial pacific experiment. *J. Atmos. Sci.* **53**, 2401–2423.

Monahan, E. C., Spiel, D. E. and Davidson, K. L. 1986. A model of marine aerosol generation via whitecaps and wave disruption. In: E. C. Monahan and G. MacNiocaill, eds., *Oceanic Whitecaps*, D. Reidel, Norwell, Mass.

Moss, S. J. and Johnson, D. W. 1994. Aircraft measurements to validate and improve numerical model parameterisations of ice to water ratios in clouds. *Atmos. Res.* **34**, 1–25.

Nordeng, T. E. 1994. Extended versions of the convective parameterization scheme at ecmwf and their impact on the mean and transient activity of the model in the tropics. Tech. Rep. 206, European Centre for Medium-Range Weather Forecasts.

Ou, S.-C. and Liou, K.-N. 1995. Ice microphysics and climatic temperature feedback. *Atmos. Res.* **35**, 127–138.

Pawlowska, H. and Brenguier, J.-L. 2000. Microphysical properties of stratocumulus clouds during ACE-2. *Tellus* **52B**, 868–887.

Pitter, R. L. and Pruppacher, H. R. 1973. A wind tunnel investigation of freezing of small water drops falling at terminal velocity in air. *Q. J. R. Meterol. Soc.* **99**, 540–550.

Pruppacher, H. R. and Klett, J. D. 1997. *Microphysics of Clouds and Precipitation*. Kluwer Acad., Norwell, Mass.

Rotstayn, L. D. 1999. Indirect forcing by anthropogenic aerosols: A global climate model calculation of the effective radius and cloud lifetime effects. *J. Geophys. Res.* **104**, 9369–9380.

Schröder, F., Kärcher, B., Petzold, A., Baumann, R., Busen, R., Hoell, C. and Schumann, U. 1998. Ultrafine aerosol particles in aircraft plumes: In situ observations. *Geophys. Res. Lett.* **25**, 2789–2792.

Ström, J. and Ohlsson, S. 1998. In situ measurements of enhanced crystal number densities in cirrus clouds caused by aircraft exhaust. *J. Geophys. Res.* **103**, 11,355–11,361.

Tiedtke, M. 1989. A comprehensive mass flux scheme for cumulus parameterization in large-scale models. *Mon. Weather Rev.* **117**, 3040–3061.

Weng, F. and Grody, N. C. 1994. Retrieval of cloud liquid water using the special sensor microwave imager (SSM/I). *J. Geophys. Res.* **99**, 25,535–25,551.

Young, K. C. 1974. A numerical simulation of wintertime, orographic precipitation; part 1, Description of model microphysics and numerical technique. *J. Atmos. Sci.* **31**, 1735–1748.

This preprint was prepared with the AGU LaTeX macros v3.1. File ice2pp formatted 2001 June 25.

With the extension package 'AGU^{++}' by P.W.Daly, version 1.5 from 1996/08/20

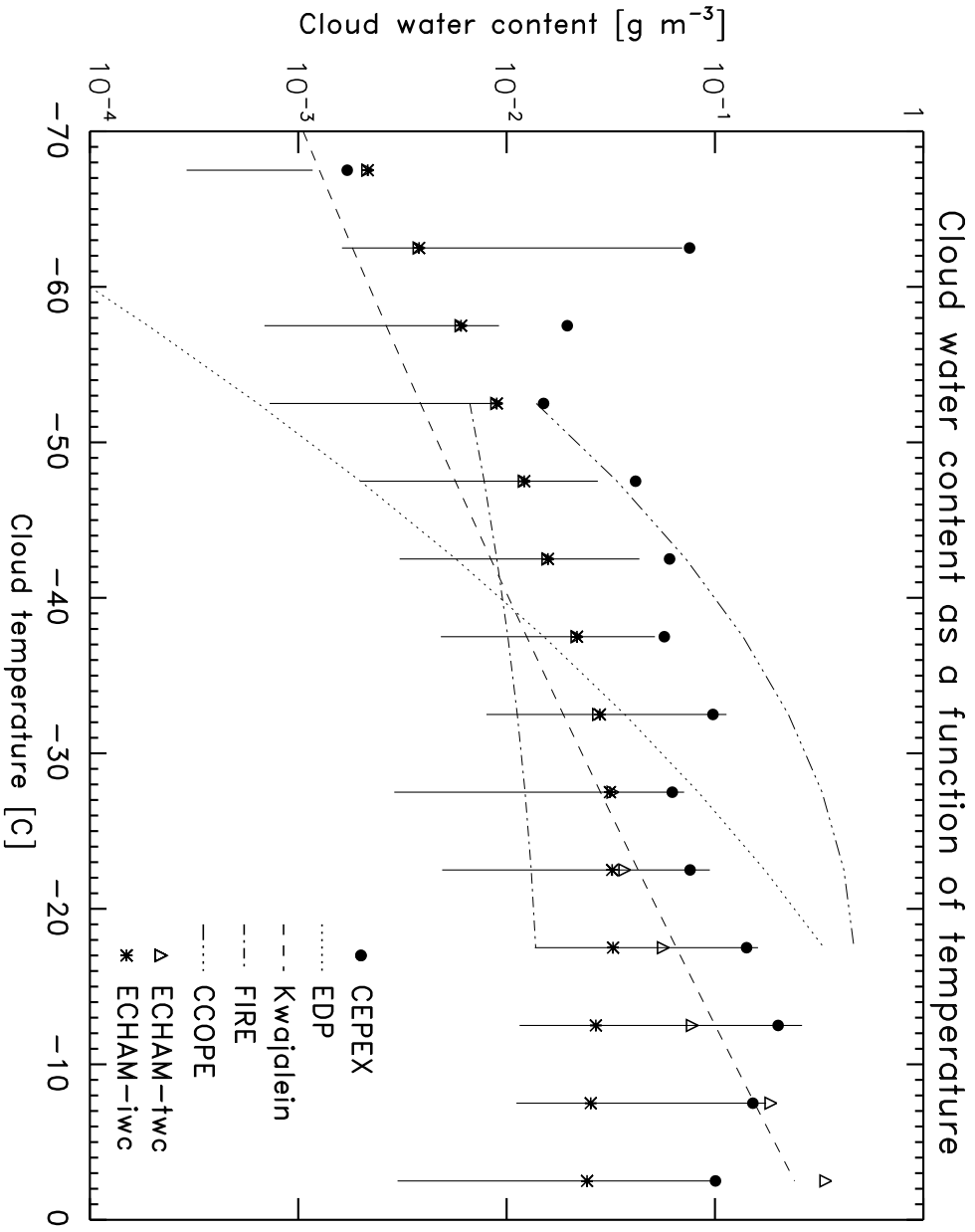

Figure 1. Cloud water content as a function of temperature for different observations and ECHAM

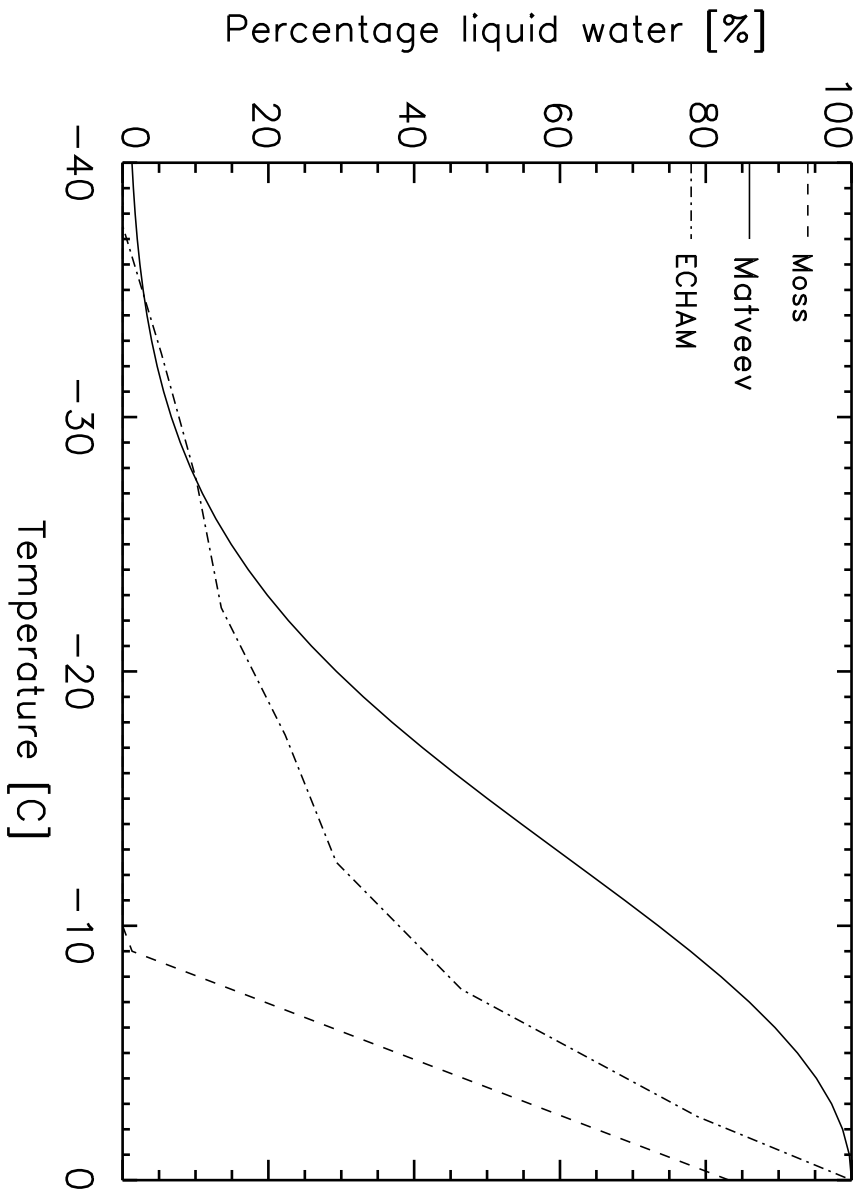

Figure 2. The fraction of cloud layers that are supercooled cloud water from different observations and ECHAM

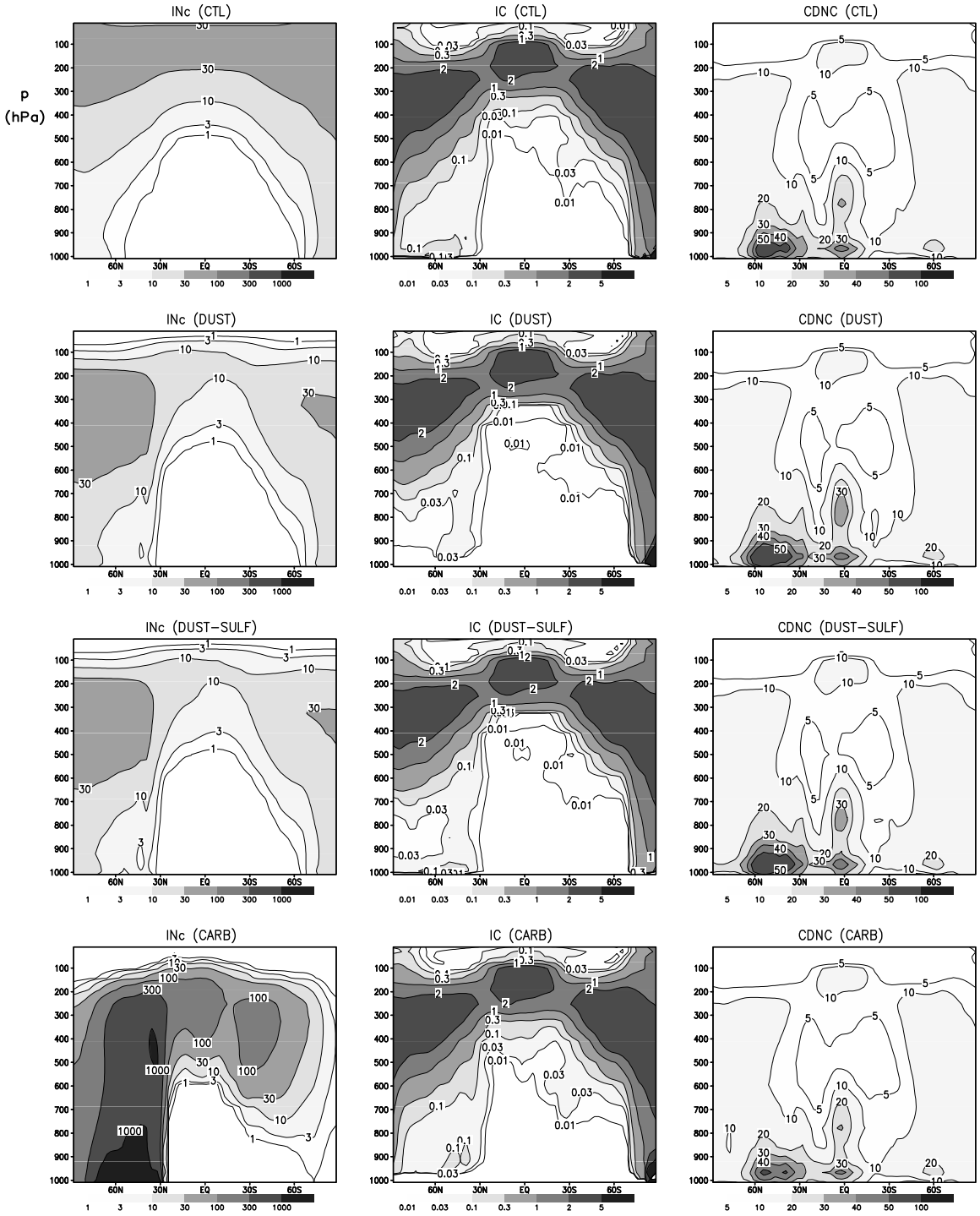

Figure 3. Annual zonal mean cross section of contact ice nuclei number concentration (INc) [cm^{-3}] (left column), ice crystal number concentration (IC) [cm^{-3}] (middle column), and cloud droplet number concentration (CDNC) [cm^{-3}] (right column) for the different simulations.

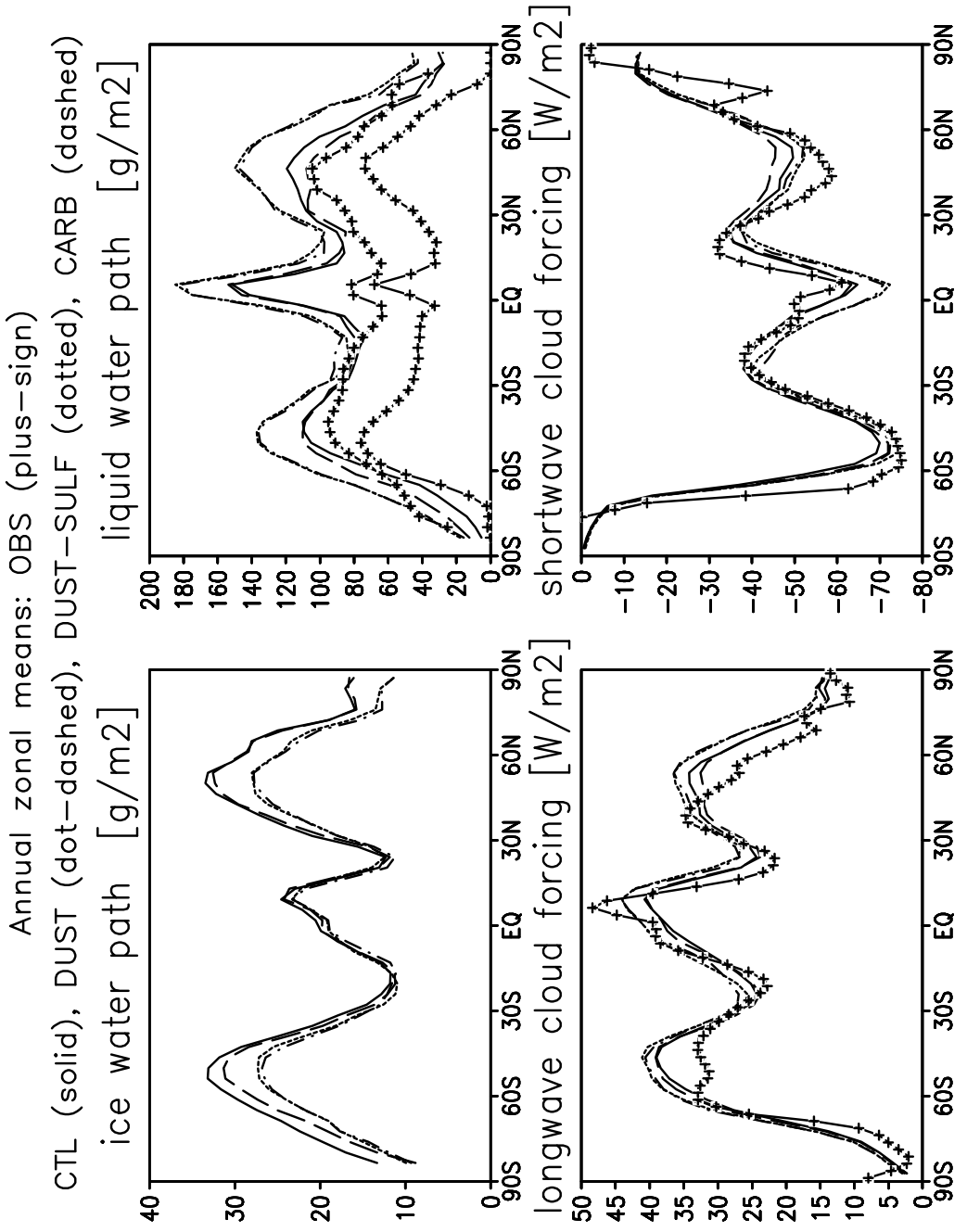

Figure 4. Annual zonal mean ice water path, liquid water path, shortwave and longwave cloud forcing from observations and ECHAM. Observational data for liquid water path are two different estimates from SSM/I and for the longwave and shortwave cloud forcing from ERBE.

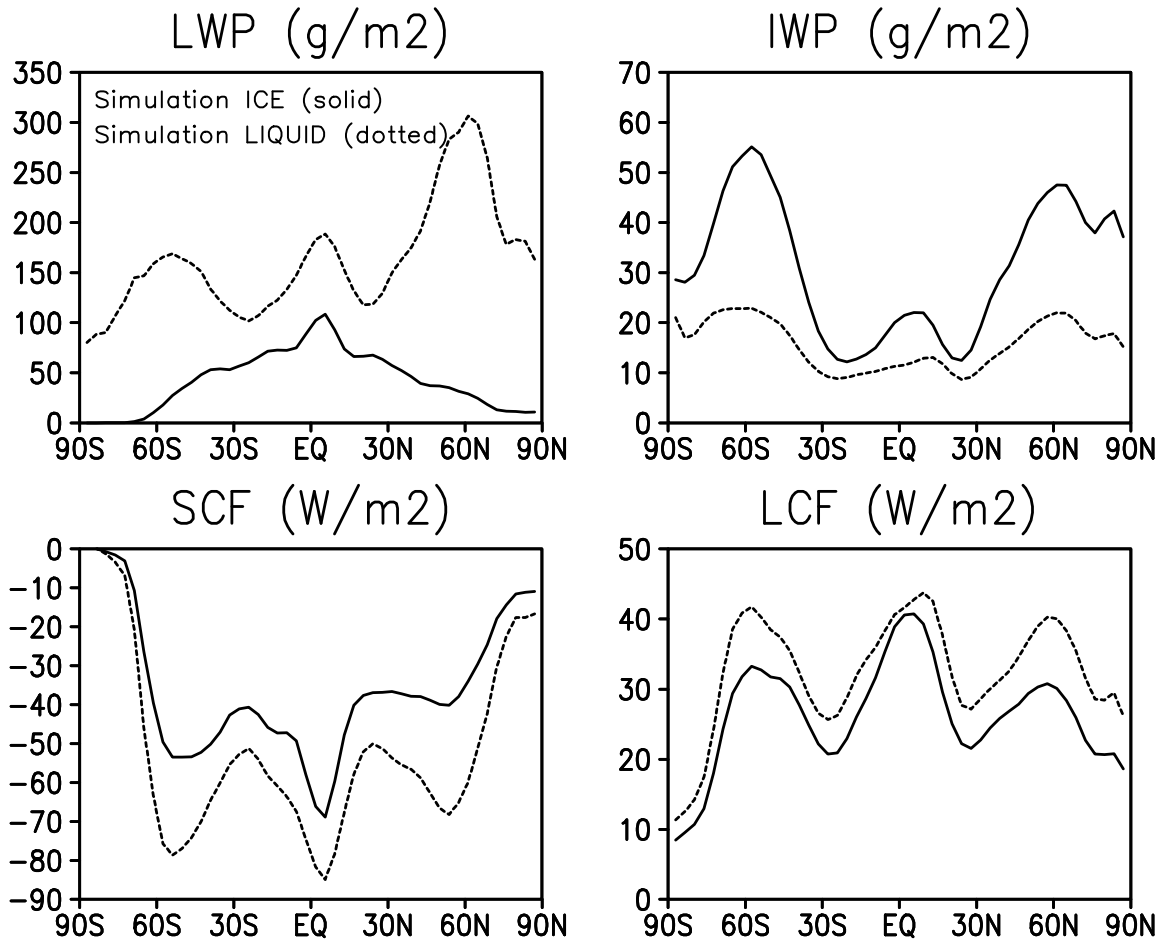

Figure 5. Annual zonal mean liquid and ice water path and shortwave and longwave cloud forcing for the simulations ICE and LIQUID